

# Experimental report

03/06/2020

**Proposal:** 9-13-806

**Council:** 10/2018

**Title:** Effect of oxidative stress on polyunsaturated lipid bilayers modulated by cholesterol and head group composition

**Research area:** Soft condensed matter

**This proposal is a new proposal**

**Main proposer:** Martin MALMSTEN

**Experimental team:** Sara MALEKKHAIAT HAFFNER

Liv Sofia Elinor DAMGAARD

Elisa Maria PARRA ORTIZ

Kathryn BROWNING

**Local contacts:** Thomas SAERBECK

**Samples:** Cholesterol  
Silicon crystals  
Quartz crystals  
hydrogenated phospholipids  
TiO<sub>2</sub> nanoparticles

Instrument	Requested days	Allocated days	From	To
FIGARO	5	0		
D17	5	4	08/07/2019	12/07/2019

## Abstract:

The oxidation of biological membranes plays key roles in pathological conditions such as inflammation, infection, or sepsis, through direct damage of the cell membrane. Oxidative stress mainly affects phospholipids with polyunsaturated acyl chains, and leads to a complex mixture of products that dramatically alter membrane properties such as 2D structure, bilayer stability, or membrane protein interactions. The roles of different cell lipid components such as cholesterol and head group species in membrane oxidation is complex and still not well understood. Interesting from a pharmaceutical point of view, the exposure of cells to photoactivatable nanomaterials such as TiO<sub>2</sub> nanoparticles (NP) induce oxidative stress, with potential application, e.g., as antimicrobial agents. Compositional differences between bacterial and mammalian membranes will likely determine their respective responses to oxidative stress. Our goal here is to use mammalian cell membrane models to elucidate structural consequences of TiO<sub>2</sub> NP-induced oxidation, the role of key membrane components such as cholesterol, PC, or PS head groups, and any potential selectivity or modulation caused by them.

## Effect of oxidative stress induced by photocatalytic titanium dioxide nanoparticles on polyunsaturated lipid bilayers

### Abstract

UV-induced membrane destabilization by TiO<sub>2</sub> nanoparticles (anatase phase) was investigated by neutron reflectometry (NR) for phospholipid bilayers formed by mixtures of 1-palmitoyl-2-oleoyl-sn-glycero-3-phosphatidylcholine (POPC), 1-palmitoyl-2-oleoyl-sn-glycero-3-phosphatidylglycerol (POPG), and 1-palmitoyl-2-arachidonoyl-sn-glycero-3-phosphocholine (PAPC). The latter is a polyunsaturated lipid very abundant in mammalian cells and tissues that hold important cellular functions and highly susceptible towards oxidation. TiO<sub>2</sub> nanoparticles display pH-dependent binding to POPC/PAPC bilayers, which is dramatically enhanced in the presence of POPG, although binding alone has virtually no destabilizing effects on the lipid bilayers. In contrast, UV illumination in the presence of TiO<sub>2</sub> nanoparticles activates membrane destabilization as a result of oxidative stress caused by generation of reactive oxygen species (ROS), primarily <sup>•</sup>OH radicals. Minor structural changes were seen by NR when TiO<sub>2</sub> was added in the absence of UV exposure, or on *in situ* UV exposure in the absence of TiO<sub>2</sub> nanoparticles. In contrast, *in situ* UV exposure in the presence of TiO<sub>2</sub> nanoparticles at high ionic strength and low pH, or in POPG-containing bilayers, caused large-scale structural transformations that we characterized in this NR experiment. These changes included gradual bilayer thinning, dramatic increases in hydration, lipid removal and potential solubilization into aggregates. These NR results, together with other data obtained by a complementary set of techniques, including small-angle X-ray scattering (SAXS), quartz crystal microbalance (QCM-D), dynamic light scattering (DLS), and ζ-potential measurements, are part of two manuscripts, one recently submitted and in revision, and another one in preparation and about to be submitted.

### Methodology

Structural features of supported POPC/PAPC bilayers (50/50 molar ratio, named as "PC") or POPC/POPG/PAPC bilayers (50/25/25 molar ratio, named as "+PG") before, during, and after exposure to UV in the absence and presence of TiO<sub>2</sub> nanoparticles at different pH and ionic strength (10 mM acetate buffer at pH 3.4, with or without 150 mM NaCl, and 10 mM Tris buffer at pH 7.4), were characterized by NR following a previously established method.<sup>1</sup> Experiments were performed on the vertical reflectometer D17 (Institut Laue-Langevin, Grenoble, France)<sup>2-3</sup> to mitigate potential bubble formation. Using two incident angles (0.8° and 3.0° in D17), the whole Q-region of interest (~0.01 to 0.3 Å<sup>-1</sup>) was covered. For kinetic measurements, an intermediate angle of 1.8° was used in order to capture the Q-region where the main changes were expected to occur, and a divergent beam geometry was set to achieve improved statistics and shorter acquisition times [29], allowing high time resolution by 60 s acquisitions. Solid-liquid flow cells, the top plate of which was modified with a 30 mm diameter circular opening, were used together with UV-transparent quartz blocks (80x50x15 mm, 1 face polished, RMS < 4.5 Å; PI-KEM Ltd., Tamworth, UK) to allow *in situ* UV irradiation (Spectroline UV lamp ENF-260C, 6 W, 254 nm; 3 mW/cm<sup>2</sup>). The supported lipid bilayers were formed by fusion of POPC/PAPC small unilamellar vesicles (done by tip sonication) onto these UV-transparent quartz substrates, rinsed in the desired buffer, and characterized in 2 contrasts (d- and h-buffer). 100 ppm TiO<sub>2</sub> nanoparticle suspensions ("+NP" samples) or equivalent buffer volumes ("-NP" samples) were subsequently injected in the cells, and the UV lamp was remotely turned on, irradiating the samples for 2 hours while simultaneously acquiring reflectivity data for the middle angle using the divergent beam geometry. The UV lamp was then turned off and the bilayers were characterized in the whole Q-region just after UV and after UV and rinsing in both d- and h-buffer contrasts.

## Results

All the initial bilayers formed at either pH 3.4 (with or without NaCl) or at pH 7.4 presented full coverages based on the low hydration levels in the tail region (~0%). In all cases, two contrasts were used, which were fitted simultaneously to a 4-slab layer model, including inner head groups, tails, and outer head groups, plus an extra water layer between the quartz surface and the inner head groups of equal roughness and thickness as the substrate roughness. In addition, a fixed head group thickness of 8 Å was assumed in order to simplify the model and to reduce the number of free parameters, a value based on previous studies.<sup>1, 4-5</sup> The model was also constrained by the requirement of the same area per molecule (APM) for the head and the tail regions<sup>1,6</sup>. Total bilayer thicknesses ( $44 \pm 1$  Å at pH 3.4;  $42 \pm 2$  Å at pH 3.4 +NaCl and pH 7.4), APM values ( $70 \pm 3$  Å<sup>2</sup> for the PC bilayers;  $66 \pm 3$  Å<sup>2</sup> for the +PG bilayer), and surface coverages ( $3.7 \pm 0.1$  mg/m<sup>2</sup> for the PC bilayers;  $3.9 \pm 0.2$  mg/m<sup>2</sup> for the +PG bilayer) were calculated.

Upon TiO<sub>2</sub> nanoparticle addition and/or *in situ* UV exposure, only minor reflectivity changes were observed for PC bilayers at low ionic strengths (10 mM, **Figure 1A**), while dramatic changes were obtained for these bilayers at high ionic strength (in the presence of 150 mM NaCl, **Figure 1B**) and for +PG bilayers in the absence of added salts (**Figure 1C**) both upon nanoparticle addition and by UV irradiation. In the absence of nanoparticles and just during and after UV exposure, very limited changes were observed in all cases.

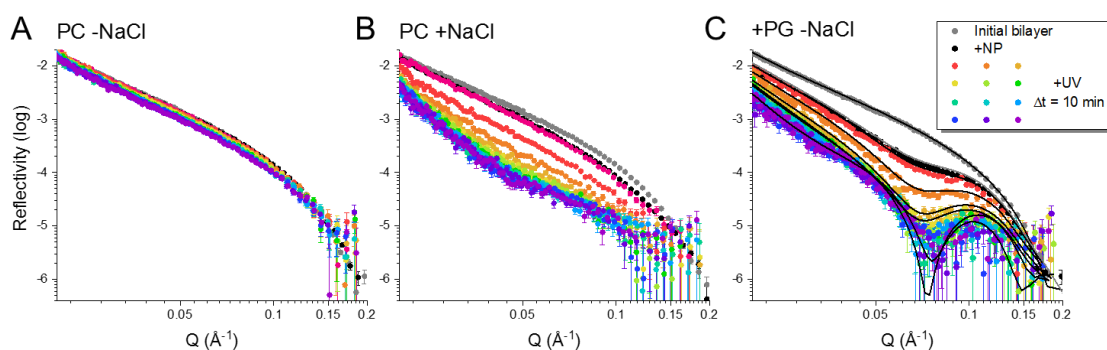


**Figure 1:** Kinetic evolution of neutron reflectivity profiles measured for supported 50/50 POPC/PAPC bilayers in the absence (**A**) or presence (**B**) of 150 mM NaCl, and for 50/25/25 POPC/PAPC/POPG bilayers (**C**), all at pH 3.4, shown before (gray) and just after (black) addition of 100 ppm TiO<sub>2</sub> NPs, as well as during *in situ* UV exposure (rainbow colours), acquired in the middle-Q region every minute using divergent beam geometry. All measurements were performed at 37°C.

All the measured reflectivity changes were analyzed in terms of changes in thickness and hydration of the different layers, while keeping constant SLD values and maintaining the constraint of equal APM for heads and tails. This was translated into increases in bilayer hydration, total APM, and decreases in surface coverage, calculated from the corresponding SLD profiles obtained from the fittings (**Figure 2**). Nevertheless, the dramatic changes observed for the PC +NaCl and the +PG -NaCl bilayer could not be explained by mere lipid removal, and instead it was necessary to modify the fitting models. For the PC +NaCl bilayer plus TiO<sub>2</sub> nanoparticles, a very thick layer with mixed SLD between the lipid head groups, acyl chains, and TiO<sub>2</sub> was formed during UV exposure on top of the progressively thinner supported bilayer (**Figure 3A and B**). The +PG bilayer in the presence of TiO<sub>2</sub> nanoparticles also needed an extra top layer, in this case with the TiO<sub>2</sub> SLD, next to a highly hydrated and partly disrupted bilayer with high APM and low surface coverage  $\Gamma$  (**Figure 3C and D**).

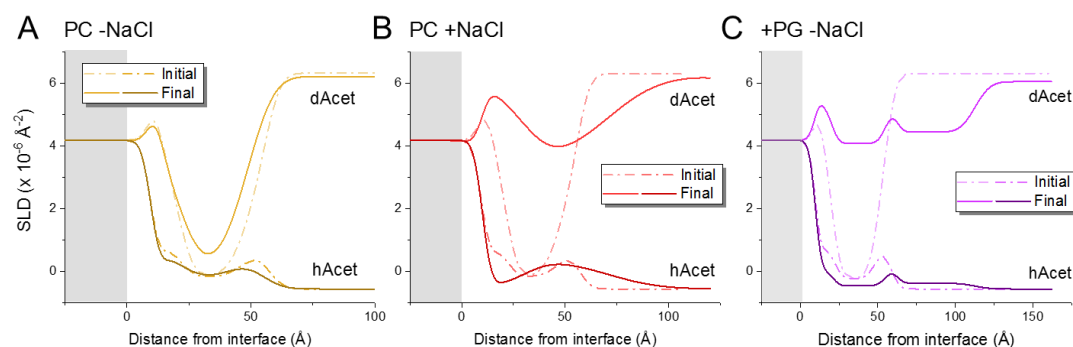


**Figure 2:** SLD profiles obtained from the fits done for the reflectivity data obtained for 2 buffer contrasts, which assumed mere lipid removal for supported 50/50 POPC/PAPC bilayers in the absence of 150 mM NaCl **(A)**; needed an extra, thick layer with mixed SLD between lipids and TiO<sub>2</sub> nanoparticles for the final PC bilayers in presence of 150 mM NaCl **(B)**; and required an extra TiO<sub>2</sub> nanoparticle layer on top of the outer head group layer for the final +PG bilayers **(C)**, all after 2 hours of *in situ* UV exposure and rinsing.

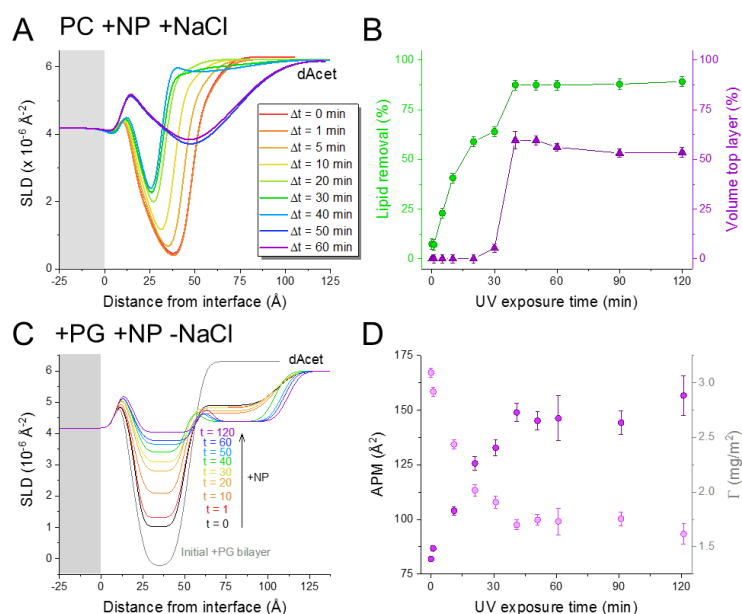


**Figure 3:** Kinetic SLD profiles and calculated changes in the physical parameters for the final PC bilayers in the presence of 150 mM NaCl **(A, B)**, and for the +PG bilayers **(C, D)**, obtained after addition of TiO<sub>2</sub> nanoparticles and after 2 hours of *in situ* UV exposure and rinsing.

## References

- Parra-Ortiz, E.; Browning, K. L.; Damgaard, L. S.; Nordström, R.; Micciulla, S.; Bucciarelli, S.; Malmsten, M., Effects of oxidation on the physicochemical properties of polyunsaturated lipid membranes. *J. Colloid Interface Sci.* **2019**, *538*, 404-419. DOI: 10.1016/j.jcis.2018.12.007.
- Cubitt, R.; Saerbeck, T.; Campbell, R. A.; Barker, R.; Gutfreund, P., An improved algorithm for reducing reflectometry data involving divergent beams or non-flat samples. *J. Appl. Crystallogr.* **2015**, *48* (6), 2006-2011. DOI: 10.1107/S1600576715019500.
- Saerbeck, T.; Cubitt, R.; Wildes, A.; Manzin, G.; Andersen, K. H.; Gutfreund, P., Recent upgrades of the neutron reflectometer D17 at ILL. *J. Appl. Crystallogr.* **2018**, *51* (2), 249-256. DOI: 10.1107/S160057671800239X.
- Kučerka, N.; Nieh, M.-P.; Katsaras, J., Fluid phase lipid areas and bilayer thicknesses of commonly used phosphatidylcholines as a function of temperature. *Biochim. Biophys. Acta, Biomembr.* **2011**, *1808* (11), 2761-2771. DOI: 10.1016/j.bbamem.2011.07.022.
- Rajamoorthi, K.; Petrache, H. I.; McIntosh, T. J.; Brown, M. F., Packing and viscoelasticity of polyunsaturated  $\omega$ -3 and  $\omega$ -6 lipid bilayers as seen by 2H NMR and X-ray diffraction. *J. Am. Chem. Soc.* **2005**, *127* (5), 1576-1588. DOI: 10.1021/ja046453b.
- Browning, K. L.; Lind, T.; Maric, S.; Malekhaiaf-Häffner, S.; Fredrikson, G.; Bengtsson, E.; Malmsten, M.; Cárdenas, M., Human lipoproteins at model cell membranes: effect of lipoprotein class on lipid exchange. *Sci. Rep.* **2017**, *7* (1), 7478. DOI: 10.1038/s41598-017-07505-0.